Available online at www.sciencedirect.com
ScienceDirect
Journal of Magnetic Resonance 182 (2006) 152–159
JMR Journal of Magnetic Resonance
www.elsevier.com/locate/jmr

Diffusion-weighted imaging with a rapid repeated hole-burning sequence

Daniel L. Weber *, Peter M. Jakob

Department of Experimental Physics 5, University of Würzburg, Am Hubland, D-97074 Würzburg, Germany

Received 27 January 2006; revised 30 May 2006
Available online 11 July 2006

Abstract

Diffusion-weighted imaging in the presence of extremely short T_2-relaxation time is generally not feasible with a standard PGSE experiment due to the superposed signal decays caused primarily by T_2-relaxation and secondarily by diffusion. Here, we present a new method for diffusion-weighted imaging achieved by a nearly T_2-independent pre-experiment where a DANTE-pulse train is repeated rapidly.

Keywords: Diffusion; DANTE; Burst; Hole-burning; Steady-state

1. Introduction

Diffusion has a strong influence on the acquired signal in MRI which can sometimes detract from image quality, but is often valuable. Simple diffusion-weighted imaging is a useful tool, for example, in the precise diagnosis of a stroke. Quantification of the diffusion coefficient in homogeneous medium is also possible, as is the acquisition of diffusion tensors, both of which provide a great deal of information about the structure of an object in an inhomogeneous medium. For instance, the characterization of neural fibers in the white matter of the brain can be carried out by measuring such parameters. In later research, other developments have emerged, such as q-space imaging, which provides information about the profile of water displacement within a single voxel on the basis of the diffusion of water molecules [1,2].

All techniques mentioned above are based on the pulsed-gradient spin-echo sequence (PGSE, [3]), where a simple spin-echo sequence is extended by adding two gradients, one before and one after the 180° refocusing pulse, which leads to diffusion encoding. The strength of the diffusion weighting in a standard PGSE experiment is given by the b-value, which depends only on the sequence parameters. The parameter b is given by

$$b = \int k(t)^2 \, \mathrm{d}t, \tag{1}$$

whereas $k(t)$ is as usual defined as

$$k(t) = \gamma \int_0^t G(\tau) \, \mathrm{d}\tau. \tag{2}$$

In the case of a PGSE sequence with rectangular, and not trapezoidal, gradient lobes, Eq. (1) becomes

$$b = \gamma^2 G^2 \delta^2 (\Delta - \delta/3), \tag{3}$$

where G is the strength of the diffusion-weighting gradient, Δ the diffusion time (the time between the initialization of the two gradients), and δ the gradient duration. For a high diffusion weighting, one needs strong and long gradients, and the time Δ between the two gradients must also be long. This long diffusion time is essential for detecting restricted diffusion in wide structures; in the case of a clinical system, long diffusion times are essential in order to obtain a suitable contrast, as the diffusion gradients that are achievable on such a system are low. Given that a long

* Corresponding author. Fax: +49 0 931 888 5851.
E-mail address: daniel.weber@physik.uni-wuerzburg.de (D.L. Weber).

1090-7807/$ - see front matter © 2006 Elsevier Inc. All rights reserved.
doi:10.1016/j.jmr.2006.06.014

diffusion time leads to a long echo time, and that the signal amplitude at the echo time is given by

$$M(\mathrm{TE}) = M_0 \cdot \exp(-\mathrm{TE}/T_2) \cdot \exp(-bD), \tag{4}$$

a high diffusion weighting is generally accompanied by a low signal amplitude. This effect is exaggerated if one wants to achieve a high diffusion weighting (high b-value) in a sample with a short T_2. Acquiring stimulated echoes can reduce, but not entirely solve, the problem of the T_2-dependence.

In 1996 Doran et al. investigated the effects of diffusion and T_1-relaxation on a rapidly repeated BURST-sequence [4]. In the sequence presented here, these effects are exploited to achieve a new kind of diffusion weighting in magnetic resonance imaging, which uses DANTE pulse trains [5] similar to well-known tagging-techniques. While this method does not have the common advantages of the BURST sequence as described in [6] or [7], advanced BURST techniques (e.g. [8]) or diffusion BURST-sequences, for example, in [9,10]—low demands on gradient power, fast, acoustically quiet—it has other desirable properties. The most obvious is that it is not affected by T_2-relaxation as are standard diffusion-weighted sequences. This is accomplished by using a pre-experiment which creates diffusion weighting using longitudinal magnetization which has been prepared by a series of DANTE-Pulses. In this technique, the generated transversal magnetization is irrelevant. The longitudinal magnetization is then read out with a fast standard experiment such as FLASH or EPI.

2. Methods

The basic idea for the method presented here comes from the Bloch–Torrey equation [11] for the longitudinal magnetization

$$\frac{\partial}{\partial t} M_z(x,t) = D \frac{\partial^2}{\partial x^2} M_z(x,t) + \frac{M_0 - M_z(x,t)}{T_1}, \tag{5}$$

which describes the evolution of the z-magnetization under the influence of diffusion and T_1-relaxation [4]. The solution of this differential equation is given below

$$M_z(x,t) = M_0 \left[1 - \exp\left(\frac{-t}{T_1}\right) \left(1 - \frac{M_z(x,0)}{M_0}\right) \otimes \frac{1}{\sqrt{4\pi D t}} \exp\left(\frac{-x^2}{4Dt}\right) \right], \tag{6}$$

where $\otimes$ symbolizes a convolution with respect to the position x [4]. In our diffusion hole-burning sequence, the z-magnetization is selectively saturated in certain locations and evolves after saturation according to diffusion and T_1-relaxation. This saturation occurs on a subvoxel level, in contrast to the diffusion measurement method using a hole-burning sequence described in [12]. To this end, several stripes are "burned" (i.e., saturated) within one voxel (Fig. 1). The pulse sequence consists of two fundamental parts:

1. Burning the stripes: z-Magnetization decreases due to saturation of several spin-ensembles.
2. Evolution: The system evolves under the influence of diffusion and T_1-relaxation. Diffusion blurs the magnetization profile, which can be described as a convolution with a normalized Gaussian kernel; this preserves the sum of the longitudinal magnetization. However, T_1-relaxation brings z-magnetization back to the positive z-axis. The evolution time T_{ev} is equivalent to the diffusion time Δ in a PGSE experiment.

If the signal of a voxel is measured after this preparation, one obtains a purely T_1-weighted image. This can be interpreted as a spatially selective saturation recovery T_1-experiment. However, if the whole procedure (burning the stripes at the same position every time, followed by evolution) is repeated again and again (L times), the amount of magnetization lost due to saturation after several repetitions is equivalent to the amount which is reclaimed due to T_1-relaxation. Thus, a steady-state is achieved, which can be read out with a fast imaging experiment. Without T_1-relaxation, the steady-state magnetization M_z^{ss} would be equal to $M_z^{ss} = 0$, because saturated spins in the pulse band would diffuse out of the pulse band, and simultaneously non-saturated spins diffuse into this band. These non-saturated spins would then be saturated in the following sequence repetition, leading to a steady-state. With T_1-relaxation alone (neglecting diffusion), repeating the pulse sequence would be unnecessary, because in every repetition the same spins would be saturated. The steady-state magnetization M_z^{ss} would be a function of T_1: $M_z^{ss} = f(T_1)$. In reality diffusion and T_1-relaxation will always co-exist, and both are needed to achieve a steady-state magnetization $M_z^{ss} > 0$ which depends on both the diffusion coefficient and the T_1-relaxation time: $M_z^{ss} = f(D, T_1)$ (Fig. 1). Because the magnetization is read out while it is in the steady-state, the diffusion weighting depends not only on sequence parameters (diffusion time, properties of the diffusion gradients) but also on the diffusion coefficient and the

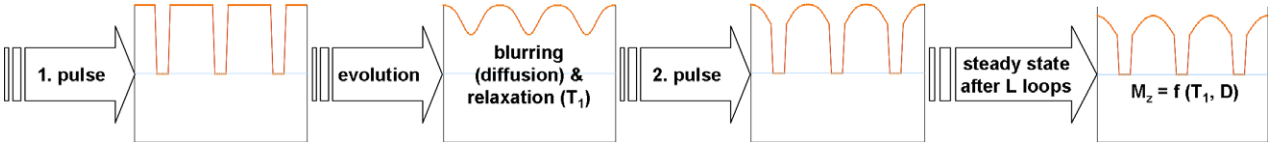

Fig. 1. The stripes burned inside a voxel are shown here. The magnetization evolves under the influence of diffusion and T_1-relaxation. After L loops of burning and evolution, a steady-state is reached.

longitudinal relaxation time themselves. This also means, however, that it is impossible to assign a single b-value for the whole image; instead, the b-values differ from voxel to voxel. The b-value can be defined by relating the magnetization without diffusion to the magnetization under the influence of diffusion:

$$b = \frac{1}{D}\ln\left(\frac{M_z^{D=0}}{M_z^{D>0}}\right) = \frac{1}{D}\ln\left(\frac{M_z^{L=0}}{M_z^{ss}(D,T_1)}\right) = b(D,T_1). \qquad (7)$$

The details of the sequence are shown in Fig. 2: Short pulses (N pulses, pulse duration τ, pulse separation Δ) are applied (generally along the x-axis of the rotation frame) under a gradient G, whose orientation defines the direction sensitive to the diffusion. Due to these pulses, the longitudinal magnetization is transformed into transversal magnetization to some extent. This magnetization is subsequently dephased with spoiler gradients. Applying a Fourier transformation yields approximately the pulse shape in the frequency domain and the spatial shape achieved after application of the gradient (Fig. 3): The pulse sequence is an infinite Dirac-comb (peak distance Δ) convoluted with a single pulse (pulse duration τ) and multiplied by a boxcar function (duration $N\Delta$). In the Fourier domain (frequency-space), that also implies an infinite Dirac-comb (peak distance $2\pi/\Delta$) multiplied by a sinc-shaped function (width between the first zero-crossings is $4\pi/\tau$) and convolved with another sinc-shaped function (width $4\pi/N\Delta$). It is important to note that we are not referring to the echoes generated in the time domain after n RF pulses; normally n pulses applied in the presence of a magnetic field gradient generates 3^{n-1} echoes in the time domain, but in the case of equidistant pulses the number of echoes is reduced to n [6]. In our case, these echoes are spoiled; we are just interested in the magnetization profile created. The stripes burned into the longitudinal magnetization due to this pulse sequence are characterized by the following parameters in the time domain:

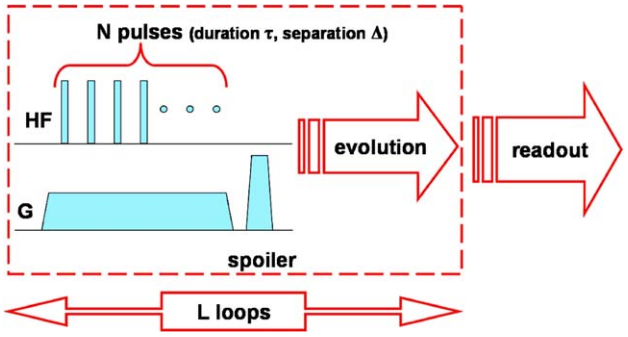

Fig. 2. N pulses are applied under a gradient G, the transversal magnetization is spoiled, and the system evolves under the influence of T_1 and diffusion. This procedure is repeated L times before the longitudinal magnetization is read out.

- The pulse distance Δ sets the distance of the stripes in the voxel: $\Delta x = 2\pi/\gamma G\Delta$. Given a certain resolution and gradient strength, the value of Δ defines the number of stripes per pixel.
- The length of one single pulse τ determines the amplitude of the stripes over the whole filed of view, which is modulated with a sinc-shaped function (see Fig. 3). The use of very short pulses is important to reach a nearly constant pulse angle over a wide area.
- The number of single pulses N controls the form and the width of one single stripe (under the condition that Δ is already determined). If the amplitude of the applied pulses is not modulated, the stripes have a nearly sinc-shaped profile with a width of $4\pi/N\Delta$. Thus, the ratio of whole width to stripe distance is given by $2/N$. Knowing the exact form of the stripes is only relevant for accurate simulation results, as the form is not important for the final image.

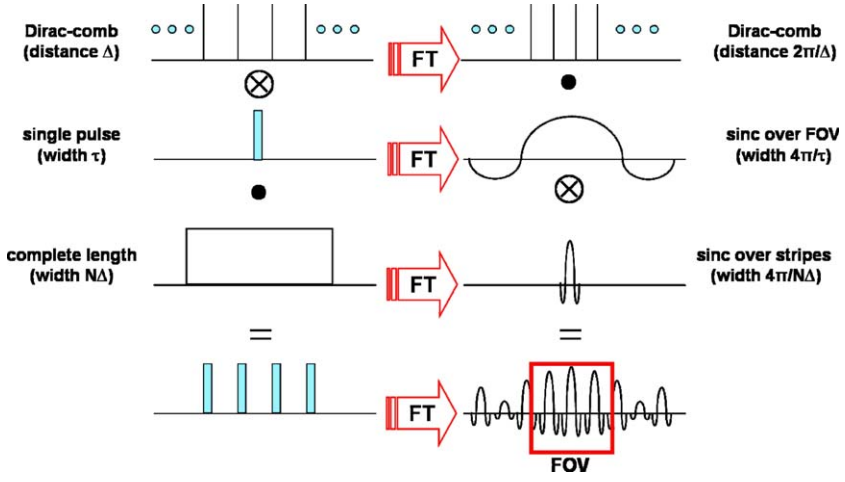

Fig. 3. The DANTE-part of the pulse-sequence (the N pulses in Fig. 2 under the curly brackets) can be approximately described as a Dirac-comb, convolved with a single block-pulse and multiplied with a boxcar-function. This leads to a Dirac-comb multiplied with a sinc-shaped function and convolved again with a sinc-shaped function in the frequency-space. A single pulse must be short enough that the amplitude of the stripes in the frequency domain is nearly homogenous over the whole field of view.

3. Simulations

For the purposes of simulating such an experiment, the system can be regarded as a one-dimensional system. The goal here is to examine one pixel containing several stripes and to simulate a 1D-line through this pixel. Assuming that the diffusion coefficient and the T_1 value do not change between two stripes inside the pixel, only a single stripe with periodic boundary conditions must be simulated. In Fig. 1 such a simulated unit cell is shown. Periodic boundary conditions mean that a spin that diffuses out of the simulated system on one side will appear on the other side. Furthermore, only z-magnetization must be taken into account. To illustrate this idea, every point in Fig. 1 represents the z-magnetization of the corresponding position.

At the beginning the system is in the steady-state. A pulse is then applied that burns one stripe, and after that the system evolves under the influence of diffusion and T_1-relaxation. This procedure is repeated periodically as described in Section 2. The simulations consist of these two parts:

1. While burning the stripes the magnetization is multiplied with a special pulse function corresponding to the position of the spins. A simple 90° pulse, for example, sets the magnetization in the pulse area to zero. To simulate short non-modulated pulses such as those used in the experiments, the z-magnetization was modified with a sinc-shaped function as described in Fig. 3. The approximation was made that the pulse occurs in one simulated time unit, during which no diffusion or T_1-relaxation takes place.
2. During the evolution of the magnetization, diffusion and T_1-relaxation modify the magnetization profile. To examine these effects, a discrete version of Eq. (5) is used:

$$\frac{\Delta M_i}{\Delta t} = D\frac{M_{i+1} + M_{i-1} - 2M_i}{\Delta x^2} + \frac{M_0 - M_i}{T_1}. \tag{8}$$

In each time step Δt the magnetization M_i at every point x_i is updated: T_1-relaxation brings longitudinal magnetization back and diffusion blurs magnetization between the actual point and the nearest neighbors (distance Δx).

The sum of all partial magnetizations M_i gives the magnetization measured in the pixel considered. Simulations were performed to find optimal experimental parameters and to check experimental results.

One interesting question is the influence of the number of stripes per pixel. Without simulations we can say that it would be desirable to have as many stripes in one pixel as possible to gain averaged information of the diffusion coefficient and the T_1-relaxation time in that pixel. This is restricted by two factors: the power of the diffusion gradient and the interval between two single short pulses which have to be very long for close stripes (see Fig. 3). So the question is not how many stripes per pixel one wants to have, but how many one can obtain.

However, it is important to find the optimal stripe width relative to the obtained stripe distance. Intuitively, it is clear that the relative stripe width must have an optimum value. If the stripes are too narrow, the hole-burning module has no effect on the readout experiment, and if the stripes are too wide, the magnetization remaining for the

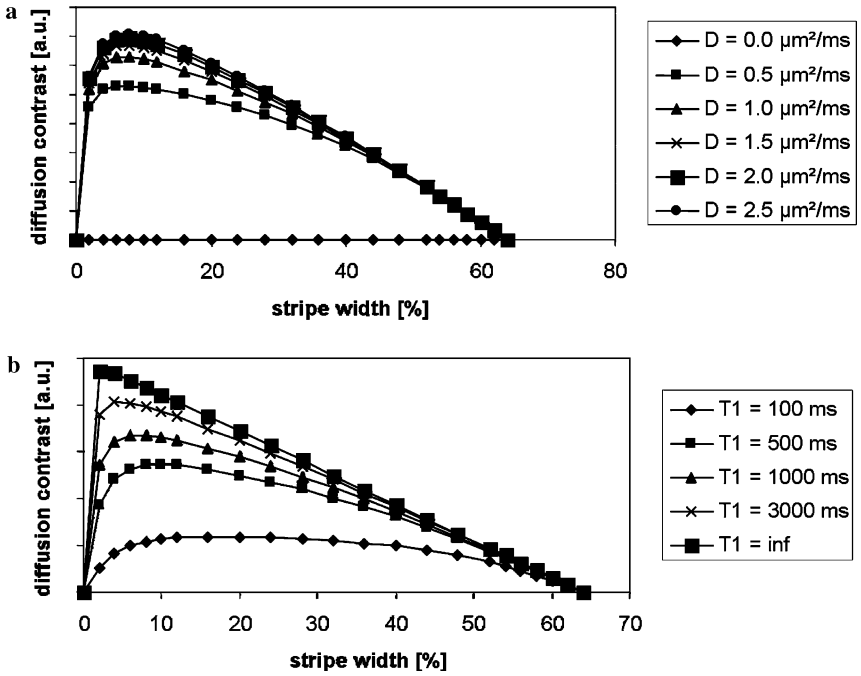

Fig. 4. (a) Diffusion contrast $M_z(D = 0) - M_z(D > 0)$ depending on the stripe width relative to the stripe distance, plotted for different values of the diffusion coefficient D. The optimal stripe width is in the range of 8–12%. Simulations are performed for $T_1 = 1000$ ms. (b) Diffusion contrast, plotted for different T_1-values and for a fixed diffusion coefficient ($D = 1.5$ µm^2/ms).

readout experiment will disappear due to diffusion and repeated burning. In Fig. 4, simulations are shown to find this optimal stripe width for rectangular stripes in dependence on D and T_1. The optimal stripe width relative to the stripe distance is between 8 and 12% for common values of D and T_1. The exact value depends on the sequence and sample parameters. This stripe width gives the best diffusion contrast, which is defined as the difference between the magnetization without diffusion $M_z(D=0)$ and the magnetization that takes diffusion into account $M_z(D>0)$.

Simulations also show that the exact form of the stripes is not essential; narrow bands of a sinc-shaped stripe profile, for example, disappear very fast due to diffusion blurring. In the presence of diffusion, nearly every stripe profile is quickly converted into a Gaussian profile.

Further simulation results are shown in Figs. 6 and 9.

4. Experimental setup

The first experiments with this hole-burning sequence were performed on a Bruker AMX-500 11.75T system due to the gradient strength of 660 mT/m. The experiments were performed using the following parameters: $\tau = 3$ μs, $\Delta = 1$ ms, $N = 25$, $T_{ev} = 25$ ms, $G = 0.45$ T/m, $\Delta x = 52$ μm, $L = 20$. For the read out, a centric reordered snapshot FLASH was used (TE = 2.5 ms, TR = 4.3 ms) with a FOV of 20×20 mm^2 and a matrix size of 128×128 pixels, generating 3 stripes per pixel. A phantom

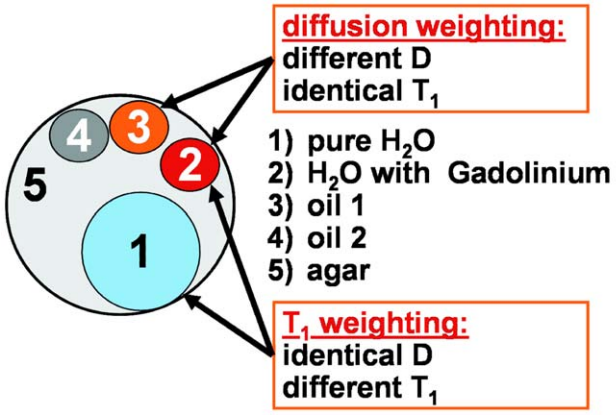

Fig. 5. The phantom was built in such a way that diffusion weighting and T_1-weighting could be separated: two tubes (2 and 3) have different diffusion coefficients but identical T_1 values (diffusion weighting), and two tubes (1 and 2) have identical diffusion coefficients but different T_1-relaxation times (T_1-weighting). The agar was used to fix the small tubes in place and to improve the ability to shim.

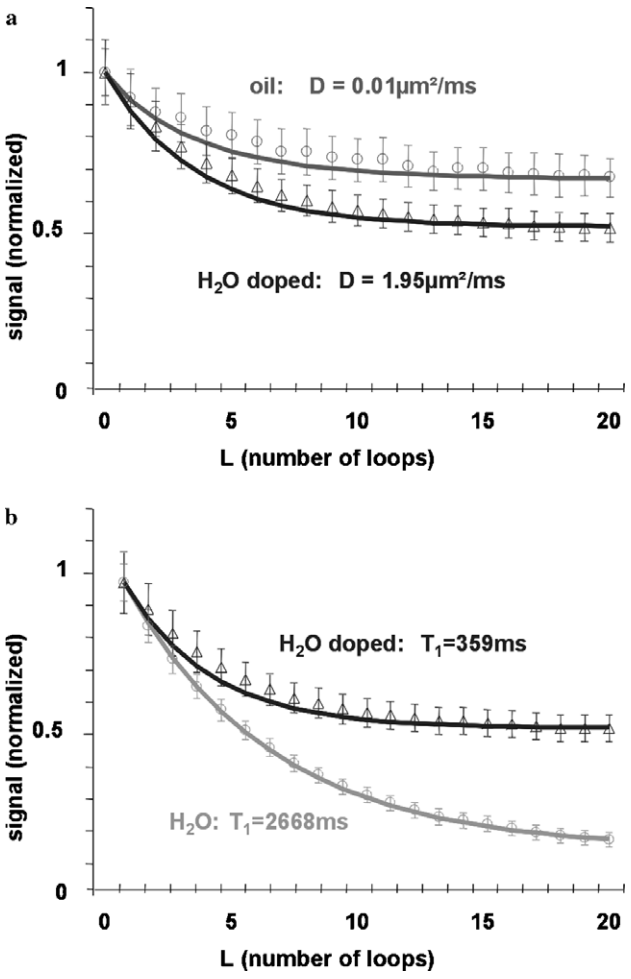

Fig. 6. (a) The signal amplitudes for the two tubes in the phantom with identical T_1-values but different diffusion coefficients after different numbers of loops are shown. The signal difference in the steady-state (large L) represents the diffusion weighting. Points are experimental data (mean values of ROIs inside the tubes), lines the results of corresponding simulations. (b) Signal amplitudes for the two tubes with identical diffusion coefficients but different T_1-relaxation times are shown. The signal difference gives the T_1-weighting. Points are experimental data, lines the results of corresponding simulations.

Table 1
This table gives an overview of the T_1 and T_2 values, the diffusion coefficients, and the calculated b-values of the phantom used for the experiments

	H_2O (1)	H_2O doped (2)	Oil 1 (3)	Oil 2 (4)
T_1 (ms)	2668 ± 70	359 ± 14	295 ± 25	327 ± 25
T_2 (ms)	535 ± 8	279 ± 7	35 ± 4	27 ± 4
D (10^{-3} mm^2/s)	1.89 ± 0.02	1.95 ± 0.05	0.01 ± 0.02	0.02 ± 0.02
b (s/mm^2)	1195 ± 274	632 ± 117	38825 ± 21575	36092 ± 21771

The numbers given in brackets correspond to the index of the compartments in Fig. 5. A map of the b-values is shown in Fig. 8. Diffusion measurements are performed at a temperature of 18 °C. The large errors in the b-values in the oil-filled tubes are caused by the errors in the diffusion coefficients in these tubes, which is not abnormally high but in the range of the coefficients themselves due to the small diffusion coefficients.

was built which allowed us to separate the signal weighting due to diffusion and T_1. It consisted of several tubes (Fig. 5): one with pure water, one with water doped with Gadolinium, and two tubes containing different oils. The water was doped in such a way that it had nearly the same T_1 as one of the oils, yielding two tubes with substances displaying identical T_1-values and different diffusion coefficients. These tubes allowed for the observation of diffusion weighting independent of the T_1 effects. At the same time the two water-filled tubes, displaying identical diffusion coefficients but different T_1-values, showed diffusion-independent T_1-weighting.

A characterization of the phantom is given in Table 1. We used an inversion recovery sequence for measuring the T_1-values, a PRESS sequence with variable echo time for the T_2-values, and a standard PGSE diffusion experiment for the diffusion coefficients.

With this phantom, a centric reordered snapshot FLASH with a readout period of 550 ms can be used for the readout due to the relatively long T_1-values of the fluids in the phantom. The contrast behaviour of a centric reordered experiment is dominated by the first few k-space lines. In the case of a probe with very short T_2 and possibly short T_1 one has to use a faster readout experiment such as EPI.

5. Experimental results

By increasing the number of sequence loops L (burning the stripes, evolution,...) the system can be driven into a steady-state. In Fig. 6, the signal progression into the steady-state, normalized to the signal strength without a pre-experiment (i.e., $L = 0$, without the hole-burning module), is shown. The phantom setup enables us to separate the diffusion- and the T_1-contrast, which yields the signal difference in the steady-state.

Phantom images at certain points in time are shown in Fig. 7a: The images are not normalized, and the diffusion weighting decreases the overall signal by increasing number of loops L. The noise level stays constant. Fig. 7b shows the same dataset as Fig. 7a, but in this case the signal is normalized to the doped water level (tube on the top right), so the noise level increases with increasing loop number L, i.e. diffusion weighting. Normal water signal (large tube) decreases relative to the doped water signal because the longer T_1-relaxation time gives a lower steady-state signal given the equal diffusion coefficients. On the other hand, the oil signal (tubes on the top left) increases with increas-

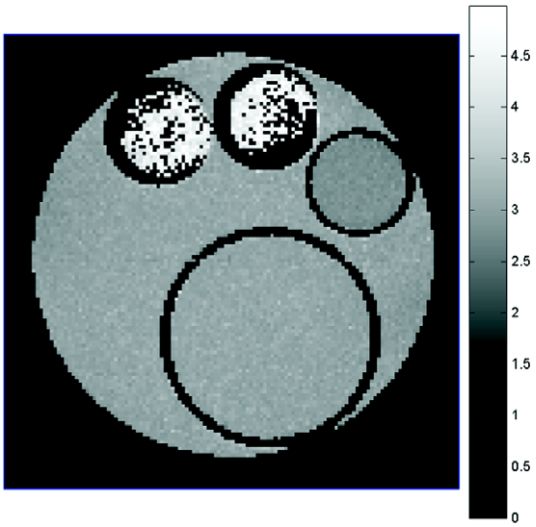

Fig. 8. Map of b-values in the phantom, calculated using Eq. (7). The scale shows the logarithm of b-values in units of s/mm^2. The sequence provides a b-value of approximately 1200 s/mm^2 ($\log_{10}(b\ \text{mm}^2/\text{s}) \approx 3.1$) for pure water (the big tube), 650 s/mm^2 ($\log_{10}(b\ \text{mm}^2/\text{s}) \approx 2.8$) for doped water (darker small tube on the right top), and nearly 40,000 s/mm^2 ($\log_{10}(b\ \text{mm}^2/\text{s}) \approx 4.6$) for oil (two bright tubes on the top).

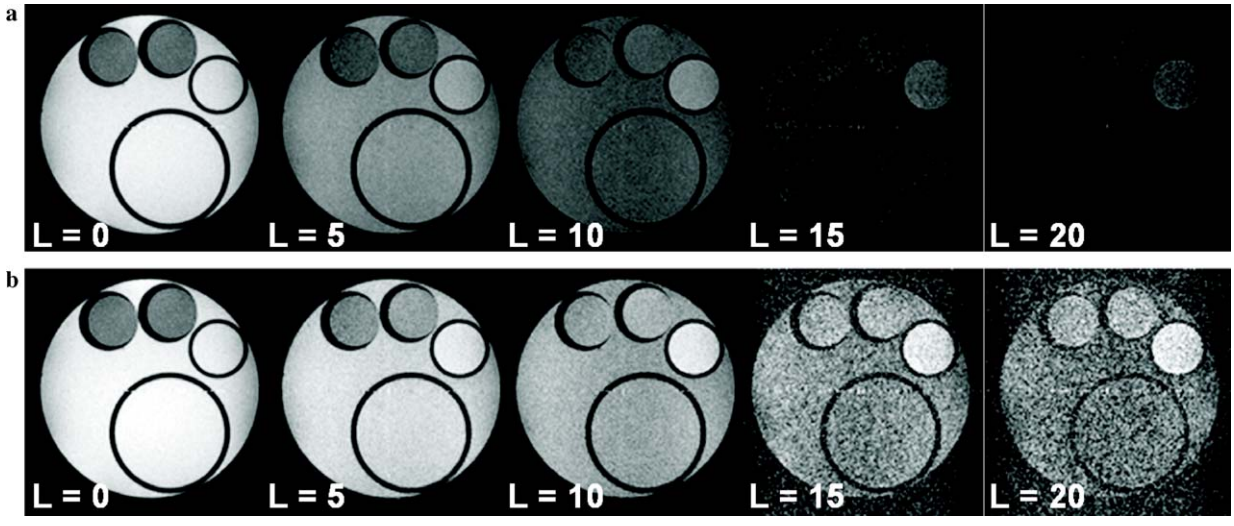

Fig. 7. (a) Signal measurements after different number of loops L. (b) The same dataset as shown in (a), but normalized to the doped water signal (tube on the top right).

ing loop number L relative to the doped water signal due to the lower diffusion coefficient at a constant T_1-relaxation time.

A map of the calculated b-values (see Eq. (7)) as shown in Fig. 8 points out the wide range of b-values achieved in a rapid repeated hole-burning sequence: With the parameters used here, pure water reaches a b-value of about 1200 s/mm^2, doped water a value of 650 s/mm^2, and oil (with its low diffusion coefficient) a b-value of approximately 40000 s/mm^2.

6. Discussion

The major advantage of rapid repeated spatial saturation in the presence of diffusion and T_1-relaxation is that it allows diffusion-weighted imaging without the signal loss caused by T_2-relaxation in samples with short T_2-relaxation times. A second advantage could be in some cases the variation of the b-value between different compartments. The dependence of the b-value from the diffusion coefficient and the T_1-relaxation time itself can permit high b-values in some cases and can also be useful in obtaining a good contrast between two areas with different D and T_1 if the contrast effects are constructive.

The contrast mixture between T_1 and diffusion contrast is problematic for a visual impression of the diffusion coefficient. For the separation of these two effects an analytical solution of the development of the steady-state magnetization $M_z^{ss}(D, T_1)$ is needed, which depends on sample properties, namely the diffusion coefficient and T_1, but also strongly on the sequence parameters. For this reason, it cannot easily be simulated. Knowing this functional relationship would provide a quantification of the diffusion coefficient and T_1 by fitting the analytical solution with the right sequence parameters to data points acquired with various loop numbers. To gain this analytical solution, one has to start with the magnetization M_0, apply one pulse, and let the system evolve (Eq. (6)). This has been done iteratively, which means that M_0 in the next step is substituted by the magnetization after the last evolution process. The steady-state magnetization $M_z^{ss}(D, T_1)$ is then given by the magnetization after an infinite number of iterations. In Fig. 9, the dependence of the simulated steady-state magnetization $M_z^{ss}(D, T_1)$ on the diffusion coefficient D and the relaxation time T_1 for a certain experimental set of parameters is shown. Both increasing diffusion coefficient and increasing T_1-relaxation time decrease the steady-state magnetization. Given common values of D and T_1 and a stripe width of approximately 10% of the stripe distance, the sequence provides a good compromise between diffusion weighting and remaining measurable signal.

A problem in contrast to a common PGSE experiment is that we have two competing lengthscales. Only if tissue properties vary on a lengthscale similar to that of the stripe distance does the method gives averaged results. Otherwise, the diffusion weighting depends only on those parts inside the pixel where the stripes are burned.

In the experiments presented here, the DANTE sequence lays down a set of stripes in the direction perpendicular to the long gradient of Fig. 2. In a heterogeneous sample, diffusion along a given stripe does not alter the magnetization profile. The only diffusion we measure by this technique is thus the component in the direction of the gradient. However, if the sample is heterogeneous, dif-

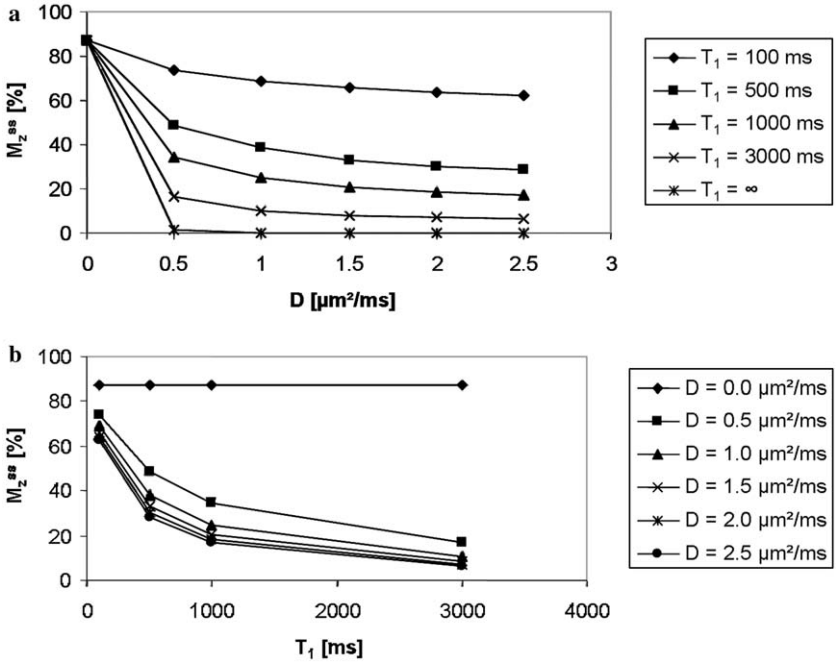

Fig. 9. (a) Simulated values of the steady-state magnetization $M_z^{ss}(D, T_1)$ immediately after the last pulse is applied. In these simulations, rectangular stripes with a stripe width of 12.5% of the stripe distance and pulse intervals of 20 ms were used. (b) Same simulations as shown in (a), but plotted over T_1 instead of D.

fusion along one part of a stripe will alter the magnetization profile of another part of that stripe. In this case, the differential equation (Eq. (5)) has to be extended to a multidimensional differential equation. However, in order to estimate the effects of the heterogeneity on the diffusion weighting, the form of the internal gradients must be known. If the heterogeneities are static and continuous, only the spin diffusion approximately perpendicular to the stripes has to be taken into account and the stripes are always burned at the same position. In that case, the sequence would give proper results, but diffusion weighting would be caused not only by the diffusion in a single direction, but by diffusion in various directions.

Working with a PGSE experiment, restricted diffusion gives an apparent diffusion coefficient or a diffusion-weighted image with a signal attenuation that is not as strong as in the unrestricted case. The same will happen here: if one has diffusion barriers in the sample, the effective diffusion coefficient is lower than the true value and thus the diffusion weighting will also be weaker.

7. Conclusion

The hole-burning sequence presented here offers a new prospect for acquiring diffusion-weighted images by preparing diffusion-weighted longitudinal magnetization. Because the transversal magnetization is not employed in this method, measurements of diffusion-weighted images are possible in T_2-ranges which are not accessible with other techniques. The diffusion weighting is achieved by repeating a spatially selective pulse train until the longitudinal magnetization enters a steady-state which depends on the diffusion coefficient and the T_1-relaxation time.

Further studies should turn the attention to the analytic calculation of the development of the steady-state magnetization $M_z^{ss}(D, T_1)$. This would provide the possibility to quantify the diffusion coefficient and possibly the T_1-relaxation time and as well as the calculation of diffusion tensor images nearly independent from T_2-effects by applying the diffusion gradient in different directions.

References

[1] P.T. Callaghan, C.D. Eccles, Y. Xia, NMR microscopy of dynamic displacements—*k*-space and *q*-space imaging, J. Phys. E: Sci. Instrum. 21 (1988) 820–822.
[2] P.T. Callaghan, D. Macgowan, K.J. Packer, et al., High-resolution *q*-space imaging in porous structures, J. Magn. Reson. 90 (1990) 177–182.
[3] E.O. Stejskal, J.E. Tanner, Spin diffusion measurements: spin echoes in the presence of a time-dependent field gradient, J. Chem. Phys. 42 (1965) 288–292.
[4] S.J. Doran, P.M. Jakob, M. Décorps, Rapid repetition of the "Burst" sequence: the role of diffusion and consequences for imaging, Magn. Reson. Med. 35 (1996) 547–553.
[5] G.A. Morris, R. Freeman, Selective excitation in Fourier transform nuclear magnetic resonance, J. Magn. Reson. 29 (1978) 433–462.
[6] J. Hennig, M. Hodapp, Burst imaging, MAGMA 1 (1993) 39–48.
[7] I.J. Lowe, R.E. Wysong, DANTE ultrafast imaging sequence (DUFIS), J. Magn. Reson. B 101 (1993) 106–109.
[8] L. Zha, I.J. Lowe, Optimized ultra-fast imaging sequence (OUFIS), Magn. Reson. Med. 33 (1995) 377–395.
[9] C.A. Wheeler-Kingshott, D.L. Thomas, M.F. Lythgoe, D. Guilfoyle, S.R. Williams, S.J. Doran, Burst excitation for quantitative diffusion imaging with multiple *b*-values, Magn. Reson. Med. 44 (2000) 737–745.
[10] S.J. Doran, M. Décorps, A. Robust, Single-shot method for measuring diffusion coefficients using the "Burst" sequence, J. Magn. Reson. A 117 (1995) 311–316.
[11] H.C. Torrey, Bloch equations with diffusion terms, Phys. Rev. 104 (1956) 563–565.
[12] E.E. Sigmund, W.P. Halperin, Hole-burning diffusion measurements in high magnetic field gradients, J. Magn. Reson. 163 (2003) 99–104.